

Stability of heterogeneous linear and nonlinear car-following models

Matthias Ehrhardt^{a,c,*}, Antoine Tordeux^{b,c}

^aUniversity of Wuppertal, Chair of Applied and Computational Mathematics,
Gaußstrasse 20, 42119 Wuppertal, Germany

^bUniversity of Wuppertal, Chair of Traffic Safety and Reliability,
Gaußstrasse 20, 42119 Wuppertal, Germany

^cInstitute for Mathematical Modelling, Analysis and Computational Mathematics,
Gaußstrasse 20, 42119 Wuppertal, Germany

Abstract

Stop-and-go waves in road traffic are complex collective phenomena with significant implications for traffic engineering, safety and the environment. Despite decades of research, understanding and controlling these dynamics remains challenging. This article examines two classes of heterogeneous car-following models with quenched disorder to shed light on the underlying mechanisms that drive traffic instability and stop-and-go dynamics. Specifically, a scaled heterogeneity model and an additive heterogeneity model are investigated, each of which affects the stability of linear and nonlinear car-following models differently. We derive general linear stability conditions which we apply to specific models and illustrate by simulation. The study provides insights into the role of individual heterogeneity in vehicle behaviour and its influence on traffic stability.

Keywords: car-following model, quenched disorder, collective stability, stop-and-go waves.

2020 Mathematics Subject Classification: 76A30, 82C22.

1. Introduction

Stop-and-go waves in road traffic are fascinating collective phenomena. Stop-and-go waves and traffic instability are observed daily around the world. They have also been observed in experiments [38, 27, 39], both with human drivers and with automated driver assistance systems (adaptive cruise control systems) [37, 13, 25]. Even deep learning approaches are being developed to dissipate stop-and-go waves [22, 16]. In addition to the scientific interest in traffic engineering, stop-and-go traffic dynamics pose important challenges for road safety and the environment. Indeed, stop-and-go dynamics lead to excessive fuel consumption and pollutant emissions compared to a uniform flow of traffic [3, 2, 37, 36].

Stop-and-go waves and traffic instability are classically addressed in traffic engineering using microscopic car-following models. Pioneering work in these areas dates back to the studies of Reuschel and Pipes early 1950s [34, 33], Chandler, Herman and co-authors late 1950s with linear

*Corresponding author

Email addresses: ehrhardt@uni-wuppertal.de (Matthias Ehrhardt), tordeux@uni-wuppertal.de (Antoine Tordeux)

models [21, 7, 14], and, later, Bando, Jiang, Treiber and co-authors with non-linear models [5, 4, 17, 47, 43]. We refer the interested reader to [52, 8, 9] for a review.

Three main factors have been identified as potential causes of stop-and-go waves:

1. **Delay and relaxation.** In fact, the introduction of a delay or relaxation in the dynamics of most car-following models leads to stability breaking. Such a feature has been noted since the 1950-1960s with linear and nonlinear models [21, 7, 12, 28] and is now a consensus in traffic engineering [26, 31, 32, 44, 42].
2. **Stochastic noise.** The first studies in this field were carried out using discrete cellular automata [6, 24, 18, 15, 35]. More recently, continuous approaches are based on Langevin and Ornstein-Uhlenbeck processes [41, 50, 46, 49, 45, 30, 51, 11, 1, 10].
3. **Individual heterogeneity.** Recent approaches show that heterogeneity in vehicle behaviour can induce stability breaking or, conversely, improve the stability of vehicle trains [37]. Heterogeneity models can be distinguished between static models lying in the agent characteristics (quenched disorder), and dynamic heterogeneity models acting in the interactions (annealed disorder) [23, 40, 19]. A general linear stability condition for heterogeneous car-following models with quenched disorder is given in [29].

Despite the large number of studies, understanding and controlling stop-and-go in road traffic flow remains challenging and still nowadays an active area of research. In particular, the role of heterogeneity and non-linearity in the shape of the model remains poorly understood.

In this article, we investigate two classes of heterogeneous car-following models with quenched disorder: a scaled heterogeneity model where a vehicle-specific factor affects the car-following model and an additive heterogeneity model, where, similar to a noisy model, an individual bias is added to the model. If the scaled heterogeneity model can affect the stability of both linear and non-linear car-following models, additive heterogeneity terms can disturb the stability of nonlinear models; this is not the case for linear models. The *full velocity difference* (FVD) model [17] and the *adaptive time gap* (ATG) model are used as reference linear and nonlinear models, respectively.

The paper is structured as follows. Next, we present the system setup, notations and a summary of the main results. The car-following models, including homogeneous, heterogeneous, linear and nonlinear models, are defined in section 2. The linear stability conditions are derived in section 3. Some simulations illustrate the results in section 4.

1.1. Setup and notations

In the sequel, we will consider $N = 3, 4, \dots$ vehicles of *length* $\ell > 0$ on a segment of length $L > N\ell$ with periodic boundaries, i.e. a circular road. We denote by $(x_n(t))_{n=1}^N$ the *positions* of the vehicles at time $t \geq 0$ and assume that the vehicles are initially ordered by their index n , i.e.,

$$0 \leq x_1(0) \leq x_2(0) \leq \dots \leq x_N(0) \leq L.$$

We assume that the predecessor of the n th vehicle is always the $(n + 1)$ th vehicle, while the predecessor of the N th vehicle is the first vehicle due to the periodic boundaries. The *distance gaps* to the predecessors are the variables

$$\begin{cases} g_n(t) = x_{n+1}(t) - x_n(t) - \ell, & n \in \{1, \dots, N - 1\}, \\ g_N(t) = L + x_1(t) - x_N(t) - \ell. \end{cases} \quad (1)$$

The *speeds* of the vehicles at time $t \geq 0$ are denoted by $(v_n(t))_{n=1}^N$, where $v_n(t) = dx_n(t)/dt = \dot{x}_n(t)$ for all $n \in \{1, \dots, N\}$. The *speed differences* with the predecessors are given by

$$\begin{cases} \Delta v_n(t) = v_n(t) - v_{n+1}(t), & n \in \{1, \dots, N-1\}, \\ \Delta v_N(t) = v_N(t) - v_1(t). \end{cases} \quad (2)$$

1.2. Summary of the results

We consider a homogeneous car-following model, defined by some universal acceleration function F , and the equilibrium gap g_e and the unique equilibrium speed v_e :

$$\dot{v}_n(t) = F(g_n(t), v_n(t), \Delta v_n(t)), \quad g_e =: L/N - \ell > 0, \quad \exists! v_e \in \mathbb{R}, \quad F(g_e, v_e, 0) = 0, \quad (3)$$

and analyze the linear stability of two types of heterogeneous dynamics, namely

1. Scaled heterogeneity model

$$\dot{v}_n(t) = a_n F(g_n(t), v_n(t), \Delta v_n(t)), \quad a_n > 0. \quad (4)$$

2. Additive heterogeneity model

$$\dot{v}_n(t) = F(g_n(t), v_n(t), \Delta v_n(t)) + b_n, \quad b_n \in \mathbb{R}. \quad (5)$$

The results show that the scaled heterogeneity factors $(a_n)_{n=1}^N$ in (4) can affect the linear stability of both linear and nonlinear car-following models F . However, the additive heterogeneity terms $(b_n)_{n=1}^N$ in (5) can only affect the stability of nonlinear models (see Table 1).

	Scaled heterogeneity model $\dot{v}_n(t) = a_n F(g_n(t), v_n(t), \Delta v_n(t))$ $a_n > 0$	Additive heterogeneity model $\dot{v}_n(t) = F(g_n(t), v_n(t), \Delta v_n(t)) + b_n$ $b_n \in \mathbb{R}$
Linear stability condition	$\frac{1}{2}f_v^2 + f_v f_{\Delta v} \geq f_g \langle 1/a \rangle$ FVD model: $\frac{1}{2}T\lambda_1 + T\lambda_2 \geq \langle 1/a \rangle$ ATG model: $\frac{1}{2}T\lambda + 1 \geq \langle 1/a \rangle$	<ul style="list-style-type: none"> • Linear model: as for the homogeneous model: $\frac{1}{2}f_v^2 + f_v f_{\Delta v} \geq f_g$ • Nonlinear model: Model specific ATG model: $\sum_{n=1}^N \frac{b_n(2\lambda T + 1)}{(b_n + \lambda v_e)^3} + \frac{\lambda^3 T v_e^2}{2(b_n + \lambda v_e)^4} \geq 0.$

Table 1: Summary of the results. Notations: $f_g = \partial_g F(g_e, v_e, 0)$, $f_v = \partial_v F(g_e, v_e, 0)$, $f_{\Delta v} = \partial_{\Delta v} F(g_e, v_e, 0)$, and $\langle 1/a \rangle = \frac{1}{N} \sum_{n=1}^N 1/a_n$. The linear *full velocity difference* (FVD) model [17] is given by $F(g, v, \Delta v) = \lambda_1(g/T - v) - \lambda_2 \Delta v$ with $\lambda_1, \lambda_2, T > 0$, while the *adaptive time gap* (ATG) nonlinear model [43] reads $F(g, v, \Delta v) = \lambda v(1 - Tv/g) - v \Delta v/g$ with $\lambda, T > 0$.

2. Car-following models and equilibrium solutions

2.1. Homogeneous car-following models

A general homogeneous car-following model reads

$$\begin{cases} \dot{x}_n(t) = v_n(t) \\ \dot{v}_n(t) = F(g_n(t), v_n(t), \Delta v_n(t)). \end{cases} \quad (6)$$

We assume that the universal acceleration function $F: \mathbb{R}^3 \mapsto \mathbb{R}$ is monotone non-decreasing with its first argument and that there exists for any $g_e = L/N - \ell > 0$ a unique equilibrium speed v_e such that

$$F(g_e, v_e, 0) = 0. \quad (7)$$

Both equilibrium gap g_e and equilibrium speed v_e are parameterised by the vehicle concentration on the segment.

FVD and ATG models. The linear *full velocity difference* (FVD) model [17] is given by

$$F(g, v, \Delta v) = \lambda_1 \left(\frac{g}{T} - v \right) - \lambda_2 \Delta v, \quad \lambda_1, \lambda_2, T > 0, \quad (8)$$

and the nonlinear *adaptive time gap* (ATG) model [43] is given by

$$F(g, v, \Delta v) = \lambda v \left(1 - \frac{Tv}{g} \right) - \frac{v \Delta v}{g}, \quad \lambda, T > 0. \quad (9)$$

For these two models, the equilibrium speed v_e is

$$v_e = \frac{g_e}{T} = \frac{L/N - \ell}{T}. \quad (10)$$

2.2. Heterogeneous car-following models

A general heterogeneous car-following model with quenched disorder reads

$$\begin{cases} \dot{x}_n(t) = v_n(t) \\ \dot{v}_n(t) = F_n(g_n(t), v_n(t), \Delta v_n(t)), \end{cases} \quad (11)$$

where the acceleration function $F_n: \mathbb{R}^3 \mapsto \mathbb{R}$ is specific to each vehicle. We assume that there exists an equilibrium solution $((g_{e,n})_{n=1}^N, v_e)$ such that

$$\begin{cases} \sum_{n=1}^N g_{e,n} = L - N\ell = N g_e, \\ F_n(g_{e,n}, v_e, 0) = 0, \quad n \in \{1, \dots, N\}. \end{cases} \quad (12)$$

In the sequel, we will consider two families of heterogeneous car-following models with quenched disorder: scaled and additive heterogeneity models.

2.2.1. Scaled heterogeneity model

The scaled heterogeneity model reads

$$\dot{v}_n(t) = a_n F(g_n(t), v_n(t), \Delta v_n(t)), \quad a_n > 0. \quad (13)$$

Here, $a_n F = 0$ implies $F = 0$ as $a_n > 0$. Therefore, the equilibrium solution of the heterogeneous model (13) matches the solution of the homogeneous model, i.e., $g_{e,n} = g_e$ for all $n \in \{1, \dots, N\}$ while v_e is the solution of the equilibrium equation $F(g_e, v_e, 0) = 0$.

2.2.2. Additive heterogeneity model

The additive heterogeneity model is given by

$$\dot{v}_n(t) = F(g_n(t), v_n(t), \Delta v_n(t)) + b_n, \quad b_n \in \mathbb{R}. \quad (14)$$

Here, the equilibrium solution satisfies the gap conservation and the equilibrium condition, i.e.

$$\begin{cases} \sum_{n=1}^N g_{e,n} = N g_e \\ F(g_{e,n}, v_e, 0) + b_n = 0, \quad n \in \{1, \dots, N\}. \end{cases} \quad (15)$$

Full velocity difference model.

Proposition 2.1. *The equilibrium state (15) of the FVD model (8) with additive bias is given by*

$$v_e = \frac{g_e}{T} + \frac{\langle b \rangle}{\lambda_1}, \quad \text{with} \quad \langle b \rangle = \frac{1}{N} \sum_{n=1}^N b_n, \quad (16)$$

and

$$g_{e,n} = g_e + \frac{T}{\lambda_1} (\langle b \rangle - b_n), \quad n \in \{1, \dots, N\}. \quad (17)$$

Proof. We obtain from (8) and (15) that $\lambda_1(g_{e,n}/T - v_e) + b_n = 0$ for all $n \in \{1, \dots, N\}$ and we can deduce

$$g_{e,n} = T \left(v_e - \frac{b_n}{\lambda_1} \right), \quad n \in \{1, \dots, N\}. \quad (18)$$

Using (18) and the gap conservation in (15), the equilibrium speed v_e is the solution of

$$\sum_{n=1}^N T \left(v_e - \frac{b_n}{\lambda_1} \right) = N g_e, \quad (19)$$

which is

$$v_e = \frac{g_e}{T} + \frac{\langle b \rangle}{\lambda_1}, \quad \langle b \rangle = \frac{1}{N} \sum_{n=1}^N b_n. \quad (20)$$

It follows from (18) that

$$g_{e,n} = T \left(\frac{g_e}{T} + \frac{\langle b \rangle}{\lambda_1} - \frac{b_n}{\lambda_1} \right) = g_e + \frac{T}{\lambda_1} (\langle b \rangle - b_n), \quad n \in \{1, \dots, N\}. \quad (21)$$

□

The equilibrium speed (16) is non-negative if

$$\langle b \rangle > -\frac{g_e \lambda_1}{T}, \quad (22)$$

while the equilibrium gaps (17) are non-negative for each vehicle if

$$\max_n b_n < \frac{g_e \lambda_1}{T} + \langle b \rangle. \quad (23)$$

Furthermore, the speed (16) matches the equilibrium speed of the homogeneous model $v_e = g_e/T$, and the equilibrium gaps (17) are

$$g_{e,n} = g_e - b_n \frac{T}{\lambda_1}, \quad n \in \{1, \dots, N\}, \quad (24)$$

if the individual bias b_n is zero in average, i.e., if $\langle b \rangle = 0$.

Remark 1 (Homogeneous case). *If the individual bias b_n is identical for all vehicles, $b_n = b$, $n \in \{1, \dots, N\}$, then the equilibrium speed (16) is*

$$v_e = \frac{g_e}{T} + \frac{b}{\lambda_1}, \quad (25)$$

while the equilibrium gaps (17) are uniform: $g_{e,n} = g_e$, $n \in \{1, \dots, N\}$.

Adaptive time gap model.

Proposition 2.2. *The equilibrium state (15) of the ATG model (9) with additive bias is given by*

$$\sum_{n=1}^N \frac{\lambda T v_e^2}{b_n + \lambda v_e} = N g_e \quad (26)$$

and

$$g_{e,n} = \frac{\lambda T v_e^2}{b_n + \lambda v_e}, \quad n \in \{1, \dots, N\}. \quad (27)$$

Proof. We obtain from (9) and (15) that $\lambda v_e(1 - T v_e/g_{e,n}) + b_n = 0$ and we can deduce

$$g_{e,n} = \frac{T v_e}{\frac{b_n}{\lambda v_e} + 1} = \frac{\lambda T v_e^2}{b_n + \lambda v_e}, \quad n \in \{1, \dots, N\}. \quad (28)$$

Using the gap conservation $\sum_{n=1}^N g_{e,n} = N g_e$, the equilibrium speed v_e is the solution of (26). \square

Let us note that the equilibrium gaps $g_{e,n}$ (27) are positive for each vehicle if

$$v_e > -\frac{1}{\lambda} \min_n b_n. \quad (29)$$

Remark 2. *We recover the equilibrium solution of the homogeneous ATG model (10)*

$$v_e = \frac{g_e}{T} \quad \text{and} \quad g_{e,n} = g_e, \quad n \in \{1, \dots, N\}, \quad (30)$$

if the biases are zero, i.e., $b_n = 0$ for all $n \in \{1, \dots, N\}$.

In the case where the individual bias is the same for all vehicles: $b_n = b$, $n \in \{1, \dots, N\}$, we have

$$\frac{\lambda T v_e^2}{b + \lambda v_e} = g_e. \quad (31)$$

Assuming $b > -\lambda v_e$ (see (29)), we obtain

$$\lambda T v_e^2 - (b + \lambda v_e) g_e = 0, \quad (32)$$

and we can deduce that (we take the positive root to make v_e positive)

$$v_e = \frac{g_e \lambda + \sqrt{(g_e \lambda)^2 + 4 \lambda T b g_e}}{2 \lambda T} = \frac{g_e}{2T} \left(1 + \sqrt{1 + \frac{4Tb}{\lambda g_e}} \right). \quad (33)$$

The equilibrium speed v_e exists if $1 + \frac{4Tb}{\lambda g_e} \geq 0$ and we obtain the condition

$$b \geq -\frac{\lambda g_e}{4T}. \quad (34)$$

Note that (34) implies the preliminary condition $b > -\lambda v_e$.

3. Linear stability analysis

3.1. General linear stability condition

The partial derivatives of the general heterogeneous car-following model (11) evaluated at the equilibrium are given by

$$f_n^g = \frac{\partial F_n}{\partial g}(g_{e,n}, v_e, 0), \quad f_n^v = \frac{\partial F_n}{\partial v}(g_{e,n}, v_e, 0), \quad f_n^{\Delta v} = \frac{\partial F_n}{\partial \Delta v}(g_{e,n}, v_e, 0). \quad (35)$$

The characteristic equation of the resulting linear ODE system reads

$$\prod_{n=1}^N [z^2 - z(f_n^v - f_n^{\Delta v}) + f_n^g] - e^{-i\theta N} \prod_{n=1}^N [-z f_n^{\Delta v} + f_n^g] = 0, \quad z \in \mathbb{C}, \theta \in [0, 2\pi]. \quad (36)$$

A sufficient general linear stability condition for which all eigenvalues z have non-positive real parts, except one equal to zero (due to the periodic boundaries), is given by [29, Eq. (5)]

$$\sum_{n=1}^N \left[\frac{1}{2} \left(\frac{f_n^v}{f_n^g} \right)^2 + \frac{f_n^v f_n^{\Delta v}}{f_n^g f_n^g} - \frac{1}{f_n^g} \right] \geq 0. \quad (37)$$

For homogeneous models with $f_n^g = f_g$, $f_n^v = f_v$, and $f_n^{\Delta v} = f_{\Delta v}$, for all $n \in \{1, \dots, N\}$, assuming $f_g > 0$, the linear stability condition (37) is given by [44, 48]

$$\frac{1}{2} f_v^2 + f_v f_{\Delta v} \geq f_g. \quad (38)$$

For instance, we have for the FVD model (8)

$$f_g = \frac{\lambda_1}{T} > 0, \quad f_v = -\lambda_1, \quad \text{and} \quad f_{\Delta v} = -\lambda_2, \quad (39)$$

and thus the linear stability condition reads [17]

$$\frac{1}{2}\lambda_1 + \lambda_2 \geq \frac{1}{T}. \quad (40)$$

In case of the ATG model (9) we have

$$f_g = \frac{\lambda}{T} > 0, \quad f_v = -\lambda, \quad \text{and} \quad f_{\Delta v} = -\frac{1}{T}, \quad (41)$$

and the linear stability condition

$$\frac{\lambda T}{2} + 1 \geq 1 \quad (42)$$

systematically holds since $\lambda, T > 0$. Indeed, the ATG model is unconditionally linearly stable, cf. [20].

3.2. Scaled heterogeneity model

Proposition 3.1. *Assuming $f_g > 0$,*

$$\frac{1}{2}f_v^2 + f_v f_{\Delta v} \geq \langle 1/a \rangle f_g, \quad \text{with} \quad \langle 1/a \rangle = \frac{1}{N} \sum_{n=1}^N \frac{1}{a_n}, \quad (43)$$

is a sufficient linear stability condition of the scaled heterogeneity model (13).

Proof. We have for the scaled heterogeneity model (13)

$$f_n^g = a_n f_g, \quad f_n^v = a_n f_v, \quad f_n^{\Delta v} = a_n f_{\Delta v}. \quad (44)$$

Using the general linear stability condition (37) with these partial derivatives allows recovering directly the condition (43). \square

Remark 3. *The condition (43) matches the linear stability condition (38) of homogeneous models if $\langle 1/a \rangle = 1$.*

The condition for the FVD model (8) reads

$$\frac{1}{2}T\lambda_1 + T\lambda_2 \geq \langle 1/a \rangle, \quad (45)$$

while the linear stability condition for the ATG model (9) is given by

$$\frac{\lambda T}{2} + 1 \geq \langle 1/a \rangle. \quad (46)$$

Values of a_n less than 1 affect negatively the stability and inversely. Due to the convexity of the inverse function, the weight of a term close to zero can be much higher than the weight of a high term. Assuming that $(a_n)_{n=1}^N$ are independent and randomly distributed according to a continuous distribution with density h on $(0, \infty)$, it is easy to check that the inverse $1/a_n$ has a density $u^2 h(1/u)$ on $(0, \infty)$. For instance, if a_n is uniformly distributed in $[1 - \kappa, 1 + \kappa]$ with $0 < \kappa < 1$, we obtain $\langle 1/a \rangle \rightarrow 1 + \kappa^2$. The scaled heterogeneity negatively affects the stability although it is symmetrically distributed around 1. Note that for this special case, the stability condition for the ATG model is asymptotically $\lambda T \geq 2\kappa$.

3.3. Additive heterogeneity model

3.3.1. Linear models

Proposition 3.2. *For linear models, the stability condition of the additive heterogeneity model (14) matches the condition (38) of homogeneous models. In other words, the additive heterogeneity does not affect the stability of linear models.*

Proof. The partial derivatives are constant for linear models even in presence of additive biases, i.e.,

$$f_n^g = f_g, \quad f_n^v = f_v, \quad f_n^{\Delta v} = f_{\Delta v}. \quad (47)$$

for all $n \in \{1, \dots, N\}$. Therefore, the stability condition for linear models is the same as the condition for homogeneous models given in (38). \square

3.3.2. Nonlinear models

By definition, the partial derivatives at equilibrium of nonlinear models depend on the equilibrium state. The equilibrium state being specific to the vehicle for the additive heterogeneity model, see (17) of (27), it turns out that the partial derivatives are heterogeneous. The dependencies with the biases depends on the nature of the nonlinear components of the model. This makes the linear stability condition model specific.

Proposition 3.3. *A sufficient linear stability condition of the ATG model (9) with additive heterogeneity (14) is given by*

$$\sum_{n=1}^N \frac{b_n(2\lambda T + 1)}{(b_n + \lambda v_e)^3} + \frac{\lambda^3 T v_e^2}{2(b_n + \lambda v_e)^4} \geq 0. \quad (48)$$

Proof. For the ATG model (9), we obtain the partial derivatives

$$f_n^g = \frac{\lambda T v_e^2}{(g_{e,n})^2}, \quad f_n^v = \lambda \left(1 - \frac{2T v_e}{g_{e,n}}\right), \quad f_n^{\Delta v} = -\frac{v_e}{g_{e,n}} \quad (49)$$

We have

$$\frac{f_n^v}{f_n^g} = \frac{\lambda \left(1 - \frac{2T v_e}{g_{e,n}}\right)}{\frac{\lambda T v_e^2}{(g_{e,n})^2}} = \frac{g_{e,n}(g_{e,n} - 2T v_e)}{T v_e^2}, \quad (50)$$

while

$$\frac{f_n^v f_n^{\Delta v}}{f_n^g f_n^g} = -\frac{\lambda \left(1 - \frac{2T v_e}{g_{e,n}}\right) \frac{v_e}{g_{e,n}}}{\frac{\lambda^2 T^2 v_e^4}{(g_{e,n})^4}} = -\frac{(g_{e,n})^2 (g_{e,n} - 2T v_e)}{\lambda T^2 v_e^3}. \quad (51)$$

The sufficient linear stability condition (37) is then given by

$$\sum_{n=1}^N \left[\frac{1}{2} \left(\frac{g_{e,n}(g_{e,n} - 2T v_e)}{T v_e^2} \right)^2 - \frac{(g_{e,n})^2 (g_{e,n} - 2T v_e)}{\lambda T^2 v_e^3} - \frac{(g_{e,n})^2}{\lambda T v_e^2} \right] \geq 0, \quad (52)$$

or again

$$\begin{aligned} \sum_{n=1}^N (g_{e,n})^2 \left[\frac{\lambda(g_{e,n} - 2Tv_e)^2}{2Tv_e^2} - \frac{g_{e,n} - 2Tv_e}{Tv_e} - 1 \right] \\ = \sum_{n=1}^N (g_{e,n})^2 \left[\frac{\lambda(g_{e,n} - 2Tv_e)^2}{2Tv_e^2} - \frac{g_{e,n} - Tv_e}{Tv_e} \right] \geq 0. \end{aligned} \quad (53)$$

Then, using $g_{e,n} = \frac{\lambda Tv_e^2}{b_n + \lambda v_e}$ and remarking that $g_{e,n} - 2Tv_e = -Tv_e \frac{2b_n + \lambda v_e}{b_n + \lambda v_e}$ while $g_{e,n} - Tv_e = -Tv_e \frac{b_n}{b_n + \lambda v_e}$, we obtain

$$\sum_{n=1}^N \left(\frac{\lambda Tv_e^2}{b_n + \lambda v_e} \right)^2 \left[\frac{\left(Tv_e \frac{2b_n + \lambda v_e}{b_n + \lambda v_e} \right)^2}{2Tv_e^2} + \frac{Tv_e \frac{b_n}{b_n + \lambda v_e}}{Tv_e} \right] \geq 0. \quad (54)$$

After simplifications (we have $\lambda, T, v_e > 0$), it follows

$$\sum_{n=1}^N \frac{1}{(b_n + \lambda v_e)^2} \left[\frac{\lambda T}{2} \left(\frac{2b_n + \lambda v_e}{b_n + \lambda v_e} \right)^2 + \frac{b_n}{b_n + \lambda v_e} \right] \geq 0, \quad (55)$$

or again

$$\sum_{n=1}^N \frac{1}{(b_n + \lambda v_e)^4} \left[\frac{\lambda T}{2} (2b_n + \lambda v_e)^2 + b_n (b_n + \lambda v_e) \right] \geq 0. \quad (56)$$

We have

$$\begin{aligned} \frac{\lambda T}{2} (2b_n + \lambda v_e)^2 + b_n (b_n + \lambda v_e) &= 2\lambda T b_n^2 + \frac{1}{2} \lambda^3 T v_e^2 + 2\lambda^2 T b_n v_e + b_n^2 + b_n \lambda v_e \\ &= b_n^2 (2\lambda T + 1) + b_n (2\lambda T + 1) \lambda v_e + \frac{1}{2} \lambda^3 T v_e^2 \\ &= b_n (2\lambda T + 1) (b_n + \lambda v_e) + \frac{1}{2} \lambda^3 T v_e^2, \end{aligned} \quad (57)$$

and the linear stability condition can be written as (48). \square

Remark 4. Note that $\lambda, T > 0$ and the model is unconditionally linearly stable if $b_n = 0$ for all $n \in \{1, \dots, N\}$. Indeed, the homogeneous ATG model is unconditionally linearly stable [20].

The stability condition (48) holds systematically if the biases $b_n \geq 0$, $n \in \{1, \dots, N\}$ are all positive. Since traffic performance is improved when the biases are positive, this gives us a way to improve the stability of platooning systems. Conversely, negative biases are needed to destabilise the system.

More precisely, the right-hand term in (48) is always positive, but the left-hand term can be negative if $b_n < 0$ and even strongly negative (potentially breaking stability) if some $b_n \xrightarrow{+} -\lambda v_e$. However, this term is offset by the positive term, which also explodes when some $b_n \xrightarrow{+} -\lambda v_e$, and even faster than the negative term (exponent 4 versus exponent 3). This suggests that moderately negative $b_n \in [-\lambda v_e, 0]$ can destabilise the system.

When all individual biases are the same, i.e., $b_n = b > -\lambda g_e/(4T)$ for all $n \in \{1, \dots, N\}$, dividing by $\lambda T v_e^2$ the last line of (57) and using (31), we obtain the linear stability condition of the ATG model

$$b \geq \frac{-\lambda^2 g_e}{4T\lambda + 2}. \quad (58)$$

The bias has to be negative and sufficiently low, especially for high λ or low T , to destabilise the system.

4. Numerical results

In this section we present some numerical results to illustrate the investigations. We focus on the linear FVD model (8) and the nonlinear ATG model (8) with additive heterogeneity (14). Indeed, theoretical results show that linear models with additive heterogeneity are systematically stable if the initial model is stable, see Proposition 3.2. However, nonlinear models such as the ATG model may be unstable for large additive biases, especially negative ones, see (48).

4.1. Numerical schemes

The car-following models are simulated using an implicit Euler scheme for the positions of the vehicles, and an explicit Euler scheme for the speeds. In both schemes the time step is $\delta t = 0.01$ s.

Full Velocity Difference Model. For the FVD model (8) with additive heterogeneity (13), the scheme for the n -th vehicle, $n \in \{1, \dots, N\}$, is given by:

$$\begin{cases} x_n(t + \delta t) = x_n(t) + \delta t v_n(t + \delta t), \\ v_n(t + \delta t) = v_n(t) + \delta t \left[\lambda_1 \left(\frac{g_n(t)}{T} - v_n(t) \right) - \lambda_2 \Delta v_n(t) + b_n \right], \end{cases} \quad (59)$$

where $T = 1$ s, $\lambda_1 = 1$ s⁻¹, $\lambda_2 = 0.5$ s⁻¹. Such a setting is such that the stability condition of the homogeneous FVD model (40) holds and is critical. The additive biases (b_1, \dots, b_N) are assumed to be initially randomly distributed on $[-5, 5]$ m/s, independent, and constant over the time. The FVD model, being linear, remains stable even in the presence of large biases (see Proposition 3.2).

Adaptive Time Gap Model. The ATG model (9) is nonlinear and has a singularity when the distance gap g is zero. However, negative gaps (i.e., collisions between the vehicles) can be expected during the simulations, especially if the model is unstable. To extend the definition of the model even in the cases where the gap is negative, we reformulate the ATG model as

$$\begin{aligned} \dot{v}_n(t) &= \lambda v_n(t) \left(1 - \frac{T v_n(t)}{g_n(t)} \right) - \frac{v_n(t) \Delta v_n(t)}{g_n(t)}, \\ &= \frac{1}{T_n(t)} (\lambda (g_n(t) - T v_n(t)) - \Delta v_n(t)), \end{aligned}$$

where

$$T_n(t) = \frac{g_n(t)}{v_n(t)}, \quad v_n(t) > 0,$$

is the time gap of the n -th vehicle, $n \in \{1, \dots, N\}$. We bound the time gap in $[T_{\min}, T_{\max}]$ using the mollifier $T_\varepsilon(g_n(t), v_n(t))$ given by

$$T_\varepsilon(g, v) = f_\varepsilon\left(T_{\min}, f_{-\varepsilon}\left(T_{\max}, \frac{g}{f_\varepsilon(0, v)}\right)\right), \quad (60)$$

where f_ε is the LogSumExp function

$$f_\varepsilon(a, b) = \varepsilon \log(\exp(a/\varepsilon) + \exp(b/\varepsilon)), \quad \varepsilon = 0.01. \quad (61)$$

The function $f_\varepsilon(a, b)$ converges to the maximum of a and b as $\varepsilon \rightarrow 0^+$, and to the minimum as $\varepsilon \rightarrow 0^-$. This smoothing of the dynamics avoids singularities when the vehicles collide or when the speed is negative. The numerical scheme for the extended ATG model with additive heterogeneity for the n -th vehicle, $n \in \{1, \dots, N\}$, is finally

$$\begin{cases} x_n(t + \delta t) = x_n(t) + \delta t v_n(t + \delta t), \\ v_n(t + \delta t) = v_n(t) + \delta t \left[\frac{\lambda(g_n(t) - T v_n(t)) - \Delta v_n(t)}{T_\varepsilon(g_n(t), v_n(t))} + b_n \right]. \end{cases} \quad (62)$$

The parameter values for the simulation are $\lambda = 0.2 \text{ s}^{-1}$, $T_{\min} = 0.1 \text{ s}$, and $T_{\max} = 4 \text{ s}$, while the desired time gap is $T = 1 \text{ s}$, as for the FVD model. The additive biases (b_1, \dots, b_N) are assumed to be initially randomly distributed on $[-1, 1] \text{ m/s}$, independent, and constant over the time. Such parameterization is such that the stability condition (48) does not hold, i.e., the ATG model (62) with additive heterogeneity is unstable.

4.2. Simulation results

The simulations are performed with 20 vehicles of length $\ell = 5 \text{ m}$ on a segment of length $L = 230 \text{ m}$ with periodic boundaries, starting from a uniform initial condition. Such a setting is similar to the scenarios of the experiments carried out in Japan in 2007 [38] and more recently in the United States [37], which show rapid formation of stop-and-go waves.

We compare the dynamics obtained with the linear FVD model, which remains stable even in the presence of acceleration biases, with the nonlinear ATG model, where the biases induce an instability. The trajectories of the vehicles over the first 200 seconds are shown in Fig. 1, while the standard deviations of the vehicle distances and speeds are shown in Fig. 2.

On the one hand, the system converges to an equilibrium with heterogeneous gaps, due to acceleration biases (b_1, \dots, b_N) , see Fig. 1, left panel. The gap deviation converges to a constant while the speed deviation converges to zero (see Fig. 2, grey curves). The biases affect the equilibrium solution. However, the FVD model, being linear, remains stable (see Proposition 3.2).

On the other hand, the biases affect both the equilibrium and the stability of the nonlinear ATG model. Indeed, the stability condition (48) no longer holds for the chosen parameter setting. The dynamics show the emergence of a stop-and-go wave (see Fig. 1, right panel), while the gap and speed standard deviations converge to a limit cycle (see Fig. 1, blue curves).

5. Conclusion

The results presented in this paper show that simple static heterogeneity mechanisms in driver behaviour (quenched disorder), here an individual additive bias in acceleration, see (13), can affect

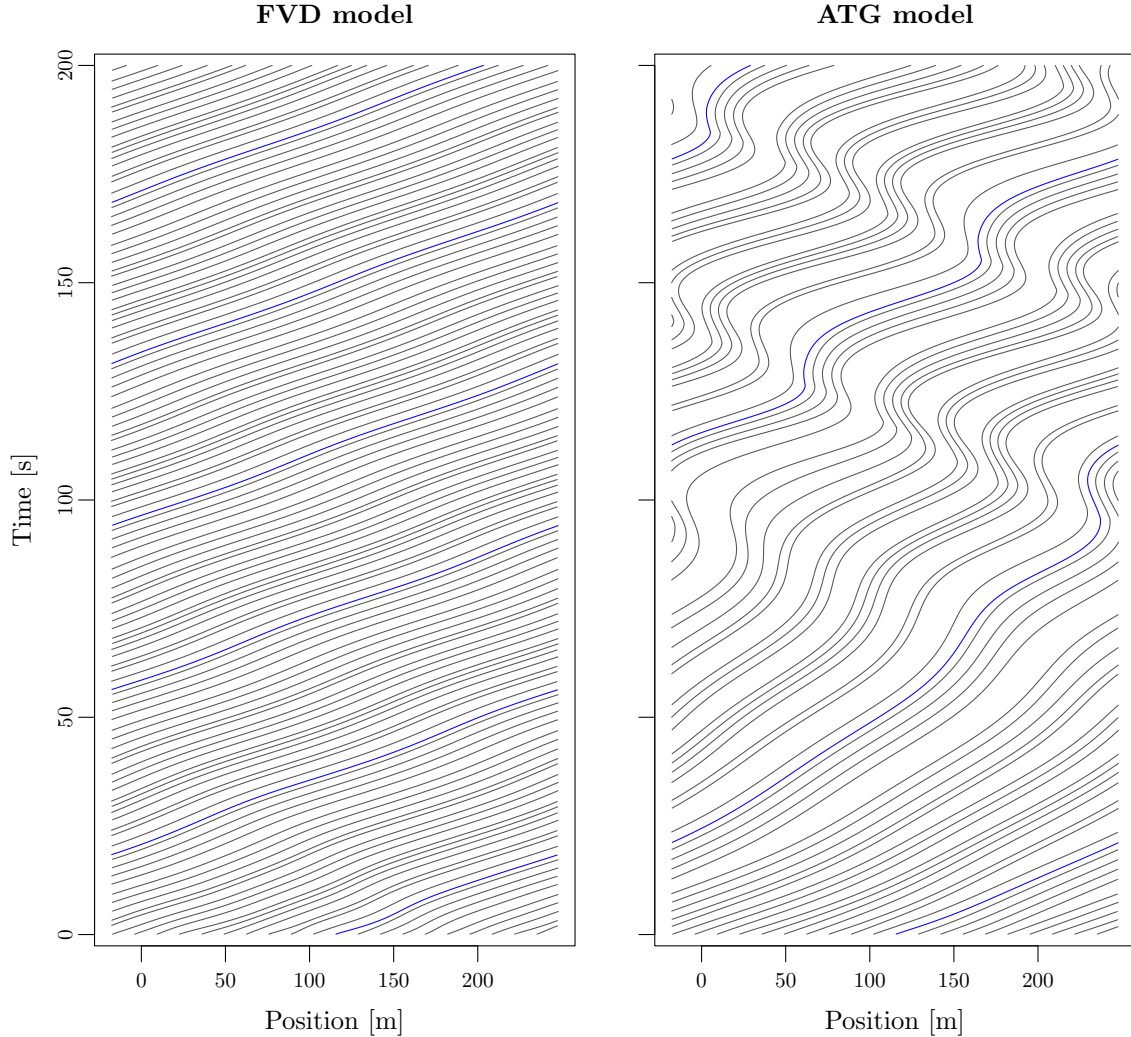


Figure 1: Trajectories of 20 vehicles on a segment of length $L = 230$ m with periodic boundaries from uniform initial conditions. Left panel: Linear FVD model (59) with additive heterogeneity (stable). Right panel: nonlinear ATG model (62) with additive heterogeneity (unstable). The FVD model remains stable even in the presence of acceleration biases and converges to an equilibrium with heterogeneous gaps, while the biases perturb the stability of the ATG model, which converges to a limit cycle with a stop-and-go wave propagating downstream.

the stability of nonlinear models and lead to the emergence of stop-and-go waves. Such a result is specific to nonlinear models, as the stability of linear models is inherently robust to additive acceleration biases. However, scalar heterogeneity models (14) can affect the stability of both linear and nonlinear models, see (43). In general, we can conclude that static heterogeneity in driver behaviour can lead to traffic instability and stop-and-go dynamics. However, other factors can also affect the stability of a line of vehicles, such as control delay, stochastic noise or, again, limited acceleration capacity. Stable car-following models and adaptive cruise controllers should consider these factors in a unified framework.

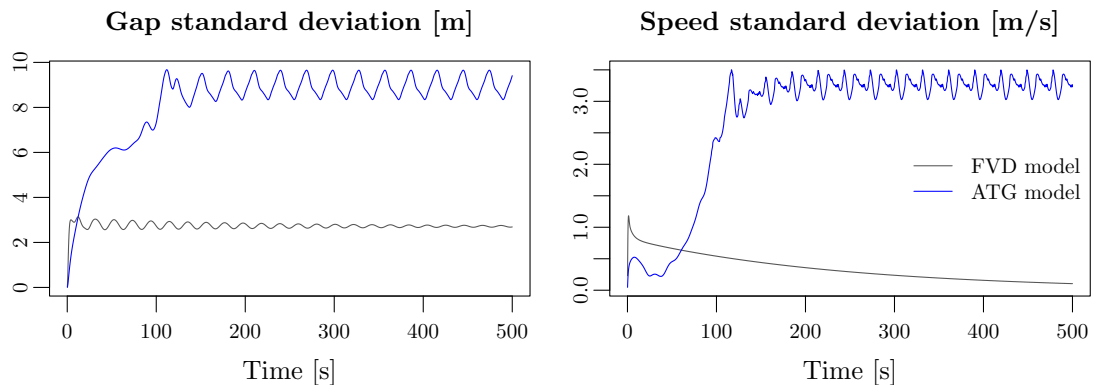


Figure 2: Time evolution of the empirical speed (left panel) and gap (right panel) standard deviations for the two scenarios shown in Fig. 1. The gap standard deviation converges and the speed standard deviation tends to zero for the stable FVD model (grey curves), while the system converges to a limit cycle with a stop-and-go wave for the unstable ATG model (blue curves).

Declarations

CRedit author statement

M. Ehrhardt: Validation, Formal analysis, Investigation, Writing – Original Draft, Writing – Review & Editing, Project administration. *A. Tordeux:* Conceptualisation, Methodology, Validation, Formal analysis, Investigation, Writing – Original Draft, Writing – Review & Editing, Software.

Data availability

All information analyzed or generated, which would support the results of this work are available in this article. No data was used for the research described in the article.

Conflict of interest

The authors declare that there are no problems or conflicts of interest between them that may affect the study in this paper.

Acknowledgements

The authors thank Oscar Dufour, Alexandre Nicolas, and David Rodney for fruitful discussions that initiated the work presented in this paper.

References

- [1] ACKERMANN, J., EHRHARDT, M., KRUSE, T., AND TORDEUX, A. Stabilisation of stochastic single-file dynamics using port-Hamiltonian systems, 2024. Accepted for publication in IFAC-PapersOnLine (26th International Symposium on Mathematical Theory of Networks and Systems).
- [2] AGUILÉRA, V., AND TORDEUX, A. A new kind of fundamental diagram with an application to road traffic emission modeling. *J. Adv. Transport.* 48, 2 (2014), 165–184.
- [3] ANDRÉ, M., AND HAMMARSTRÖM, U. Driving speeds in Europe for pollutant emissions estimation. *Transport. Res. Part D: Transp. Environ.* 5, 5 (2000), 321–335.

- [4] BANDO, M., HASEBE, K., NAKANISHI, K., AND NAKAYAMA, A. Analysis of optimal velocity model with explicit delay. *Phys. Rev. E* 58, 5 (1998), 5429.
- [5] BANDO, M., HASEBE, K., NAKAYAMA, A., SHIBATA, A., AND SUGIYAMA, Y. Dynamical model of traffic congestion and numerical simulation. *Phys. Rev. E* 51, 2 (1995), 1035–1042.
- [6] BARLOVIC, R., SANTEN, L., SCHADSCHNEIDER, A., AND SCHRECKENBERG, M. Metastable states in cellular automata for traffic flow. *Euro. Phys. J. B* 5 (1998), 793–800.
- [7] CHANDLER, R., HERMAN, R., AND MONTROLL, E. Traffic dynamics: studies in car following. *Oper. Res.* 6, 2 (1958), 165–184.
- [8] CORDES, J. Modeling of Stop-and-Go Waves in Pedestrian Dynamics, 2020.
- [9] CORDES, J., CHRAIBI, M., TORDEUX, A., AND SCHADSCHNEIDER, A. Single-file pedestrian dynamics: a review of agent-following models. *Crowd Dynamics, Volume 4: Analytics and Human Factors in Crowd Modeling* (2023), 143–178.
- [10] EHRHARDT, M., KRUSE, T., AND TORDEUX, A. The collective dynamics of a stochastic port-Hamiltonian self-driven agent model in one dimension. *ESAIM: Math. Model. Numer. Anal.* 58 (2024), 515–544.
- [11] FRIESEN, M., GOTTSCHALK, H., RÜDIGER, B., AND TORDEUX, A. Spontaneous wave formation in stochastic self-driven particle systems. *SIAM J. Appl. Math.* 81, 3 (2021), 853–870.
- [12] GAZIS, D., HERMAN, R., AND ROTHERY, R. Nonlinear follow-the-leader models of traffic flow. *Oper. Res.* 9, 4 (1961), 545–567.
- [13] GUNTER, G., GLOUDEMANS, D., STERN, R., ET AL. Are commercially implemented adaptive cruise control systems string stable? *IEEE Trans. Intell. Transport. Systems* 22, 11 (2020), 6992–7003.
- [14] HERMAN, R., MONTROLL, E., POTTS, R. B., AND ROTHERY, R. Traffic dynamics: Analysis of stability in car following. *Oper. Res.* 7, 1 (1959), 86–106.
- [15] HUANG, Y.-X., GUO, N., JIANG, R., AND HU, M.-B. Instability in car-following behavior: new Nagel-Schreckenberg type cellular automata model. *J. Stat. Mech.: Theory Exper.* 2018, 8 (2018), 083401.
- [16] JIANG, L., XIE, Y., WEN, X., CHEN, D., LI, T., AND EVANS, N. Dampen the stop-and-go traffic with connected and automated vehicles – a deep reinforcement learning approach. In *2021 7th International Conference on Models and Technologies for Intelligent Transportation Systems (MT-ITS)* (2021), IEEE, pp. 1–6.
- [17] JIANG, R., WU, Q., AND ZHU, Z. Full velocity difference model for a car-following theory. *Phys. Rev. E* 64 (2001), 017101.
- [18] KAUPUŽS, J., MAHNKE, R., AND HARRIS, R. Zero-range model of traffic flow. *Phys. Rev. E* 72, 5 (2005), 056125.
- [19] KHELFA, B., KORBMACHER, R., SCHADSCHNEIDER, A., AND TORDEUX, A. Heterogeneity-induced lane and band formation in self-driven particle systems. *Scientific reports* 12, 1 (2022), 4768.
- [20] KHOUD, P., WILL, P., TORDEUX, A., AND GRONWALD, F. Extending the adaptive time gap car-following model to enhance local and string stability for adaptive cruise control systems. *J. Intell. Transport. Syst.* (2021), 1–21.
- [21] KOMETANI, E., AND SASAKI, T. On the stability of traffic flow (Report-I). *J. Oper. Res. Soc. Japan* 2, 1 (1958), 11–26.
- [22] KREIDIEH, A., WU, C., AND BAYEN, A. Dissipating stop-and-go waves in closed and open networks via deep reinforcement learning. In *2018 21st International Conference on Intelligent Transportation Systems (ITSC)* (2018), IEEE, pp. 1475–1480.
- [23] KRÜSEMANN, H., GODEC, A., AND METZLER, R. First-passage statistics for aging diffusion in systems with annealed and quenched disorder. *Phys. Rev. E* 89, 4 (2014), 040101.
- [24] LI, K.-P., AND GAO, Z.-Y. Noise-induced phase transition in traffic flow*. *Commun. Theor. Phys.* 42, 3 (sep 2004), 369.
- [25] MAKRIDIS, M., MATTAS, K., ANESIADOU, A., AND CIUFFO, B. OpenACC. an open database of car-following experiments to study the properties of commercial ACC systems. *Transport. Res. Part C: Emerg. Techn.* 125 (2021), 103047.
- [26] NAGATANI, T., AND NAKANISHI, K. Delay effect on phase transitions in traffic dynamics. *Phys. Rev. E* 57, 6 (1998), 6415.
- [27] NAKAYAMA, A., FUKUI, M., KIKUCHI, M., ET AL. Metastability in the formation of an experimental traffic jam. *New J. Phys.* 11, 8 (2009), 083025.
- [28] NEWELL, G. Nonlinear effects in the dynamics of car following. *Oper. Res.* 9, 2 (1961), 209–229.
- [29] NGODUY, D. Effect of the car-following combinations on the instability of heterogeneous traffic flow. *Transportmetrica B: Transport Dyn.* 3, 1 (2015), 44–58.
- [30] NGODUY, D., LEE, S., TREIBER, M., KEYVAN-EKBATANI, M., AND VU, H. Langevin method for a continuous

- stochastic car-following model and its stability conditions. *Transport. Res. Part C: Emerg. Techn.* 105 (2019), 599–610.
- [31] OROSZ, G., WILSON, R., AND KRAUSKOPF, B. Global bifurcation investigation of an optimal velocity traffic model with driver reaction time. *Phys. Rev. E* 70, 2 (2004), 026207.
- [32] OROSZ, G., WILSON, R., AND STÉPÁN, G. Traffic jams: dynamics and control. *Phil. Trans. Royal Soc. A: Math., Phys. Engrg. Sci.* 368, 1928 (2010), 4455–4479.
- [33] PIPES, L. An operational analysis of traffic dynamics. *J. Appl. Phys.* 24, 3 (1953), 274–281.
- [34] REUSCHEL, A. Fahrzeugbewegungen in der Kolonne. *Österreichisches Ingenieur Archiv* 4 (1950), 193–215.
- [35] SCHADSCHNEIDER, A., CHOWDHURY, D., AND NISHINARI, K. *Stochastic Transport in Complex Systems. From Molecules to Vehicles*. Elsevier, 2010.
- [36] STERN, R., CHEN, Y., CHURCHILL, M., ET AL. Quantifying air quality benefits resulting from few autonomous vehicles stabilizing traffic. *Transport. Res. Part D: Transp. Environm.* 67 (2019), 351–365.
- [37] STERN, R. E., CUI, S., DELLE MONACHE, M., ET AL. Dissipation of stop-and-go waves via control of autonomous vehicles: Field experiments. *Transport. Res. Part C: Emerg. Techn.* 89 (2018), 205–221.
- [38] SUGIYAMA, Y., FUKUI, M., KIKUCHI, M., ET AL. Traffic jams without bottlenecks-experimental evidence for the physical mechanism of the formation of a jam. *New J. Phys.* 10, 3 (2008), 033001.
- [39] TADAKI, S.-I., KIKUCHI, M., FUKUI, M., ET AL. Phase transition in traffic jam experiment on a circuit. *New J. Phys.* 15, 10 (2013), 103034.
- [40] TATEISHI, A., RIBEIRO, H., SANDEV, T., PETRESKA, I., AND LENZI, E. Quenched and annealed disorder mechanisms in comb models with fractional operators. *Phys. Rev. E* 101, 2 (2020), 022135.
- [41] TOMER, E., SAFONOV, L., AND HAVLIN, S. Presence of many stable nonhomogeneous states in an inertial car-following model. *Phys. Rev. Lett.* 84, 2 (2000), 382.
- [42] TORDEUX, A., COSTESEQUE, G., HERTY, M., AND SEYFRIED, A. From traffic and pedestrian follow-the-leader models with reaction time to first order convection-diffusion flow models. *SIAM J. Appl. Math.* 78, 1 (2018), 63–79.
- [43] TORDEUX, A., LASSARRE, S., AND ROUSSIGNOL, M. An adaptive time gap car-following model. *Transport. Res. Part B: Method.* 44, 8-9 (2010), 1115–1131.
- [44] TORDEUX, A., ROUSSIGNOL, M., AND LASSARRE, S. Linear stability analysis of first-order delayed car-following models on a ring. *Phys. Rev. E* 86, 3 (2012), 036207.
- [45] TORDEUX, A., AND SCHADSCHNEIDER, A. White and relaxed noises in optimal velocity models for pedestrian flow with stop-and-go waves. *J. Phys. A: Math. Theor.* 18 (2016), 185101.
- [46] TREIBER, M., AND HELBING, D. Hamilton-like statistics in onedimensional driven dissipative many-particle systems. *Euro. Phys. J. B* 68 (2009), 607–618.
- [47] TREIBER, M., HENNECKE, A., AND HELBING, D. Congested traffic states in empirical observations and microscopic simulations. *Phys. Rev. E* 62, 2 (2000), 1805–1824.
- [48] TREIBER, M., AND KESTING, A. Traffic flow dynamics. *Traffic Flow Dyn.: Data, Mod. Simul.* (2013), 983–1000.
- [49] TREIBER, M., AND KESTING, A. The intelligent driver model with stochasticity-new insights into traffic flow oscillations. *Transport. Res. Proc.* 23 (2017), 174–187.
- [50] WAGNER, P. A time-discrete harmonic oscillator model of human car-following. *Euro. Phys. J. B* 84 (2011), 713–718.
- [51] WANG, Y., LI, X., TIAN, J., AND JIANG, R. Stability analysis of stochastic linear car-following models. *Transport. Sci.* 54, 1 (2020), 274–297.
- [52] WILSON, R., AND WARD, J. Car-following models: Fifty years of linear stability analysis – a mathematical perspective. *Transport. Plan. Techn.* 34, 1 (2011), 3–18.